

Length-dependent Raman spectroscopy of single-walled carbon nanotubes: the effect of dispersant on defects

J. R. Simpson,^{1,2,*} J. A. Fagan,³ M. L. Becker,³ E. K. Hobbie,³ and A. R. Hight Walker²

¹ Department of Physics, Astronomy, and Geosciences, Towson University, Towson, MD 21252, USA.

² Physics Laboratory, National Institute of Standards and Technology, Gaithersburg, MD 20899, USA.

³ Materials Science and Engineering Laboratory,

National Institute of Standards and Technology, Gaithersburg, MD 20899 USA.

(Dated: November 2, 2008)

We compare Raman spectra from aqueous suspensions of length-separated single-walled carbon nanotubes (SWCNTs) dispersed using either polymer adsorption or single-stranded DNA or miscelle encapsulation with sodium deoxycholate surfactant. The Raman spectral features, other than the D-band, increase monotonically with nanotube length in both dispersion schemes. The intensity ratio of the disorder-induced D to G' Raman bands decays as a function of SWCNT length, proportional to $1/L$, as expected for endcap defects. While the UV-vis absorption and fluorescence also increase with length for both dispersants, the fluorescence intensity is dramatically lower for DNA-wrapped SWCNTs of equal length. The similarities in the length-dependent D/G' ratios exclude defects as an explanation for the fluorescence decrease in DNA versus deoxycholate dispersions.

PACS numbers: 78.67.Ch, 78.30.Na

Applications of single-walled carbon nanotubes (SWCNTs) require an understanding of their intrinsic characteristics and sample quality. Recently, highly-purified SWCNTs have been produced that show substantial property improvement over unsorted materials.[1] However, many of the separation schemes, whether for electronic type or length, rely on different agents to aid in the dispersion of individual SWCNTs prior to separation. In this letter, we address the possible effect of the dispersing agent on the fundamental SWCNT optical characteristics, in particular the Raman scattering, either through interaction with the nanotube structure or from inherent processing differences. We accomplish this by comparing length-separated fractions of the same nanotube batch dispersed with two methods: polymer adsorption of single-stranded DNA or miscelle encapsulation with sodium deoxycholate surfactant.

DNA-wrapped CoMoCat SWCNTs (S-P95-02 Grade, Batch NI6-A001, Southwest nanotechnologies) were prepared using (GT)₁₅ single-stranded DNA and separated by length using size exclusion chromatography (SEC).[2, 3] Sodium deoxycholate (DOC) dispersions of SWCNTs from the same CoMoCat starting material were prepared by substituting DOC (2% by mass) for the DNA. These DOC dispersions were length separated via centrifugation.[4] The resulting samples, which are well-dispersed and length-separated fractions, exhibit insignificant chirality enhancement. After length separation, these aqueous samples are then concentrated and dialyzed to remove non-SWCNT components, apart from the dispersants.

Raman spectra were collected from fractions ranging in length from approximately 60 nm to larger than 1 μm . For optical characterization by UV-vis transmission and NIR fluorescence, we focus on two sets of length frac-

tions, denoted *A* and *B*, with nearly identical lengths for the different dispersions of approximately $L_A = 580$ nm and $L_B = 230$ nm. Figure 1 shows a comparison of the Raman spectra measured for different length fractions dispersed with DOC surfactant. The spectral intensities

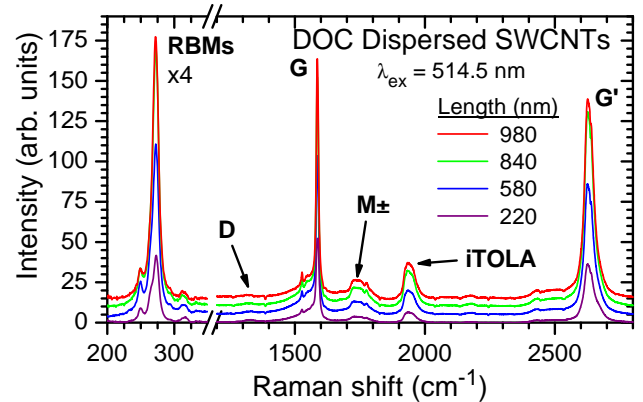


FIG. 1: Raman scattering from DOC dispersed SWCNT fractions with laser excitation at 514.5 nm, and scaled by the water OH-stretch mode (not shown) for concentration. SWCNT phonon modes are indicated. The D-band ($\approx 1328 \text{ cm}^{-1}$) is relatively constant in length and substantially smaller than the RBM (scaled 4 \times), G, and G' peaks, all of which increase in intensity with length.

are scaled for SWCNT concentration[5] by the strength of the water OH-stretch mode at $\approx 3400 \text{ cm}^{-1}$. The scattering intensity (each spectrum offset 5 units for clarity) increases monotonically with the length of the fractions. With laser excitation at 514.5 nm, strong features due to the radial breathing modes (RBMs), G, G', iTOLA, and M \pm -bands[6] are clearly visible. The RBM spectral region shown in Fig. 1 is scaled by a factor of four.

Figure 2(a) shows for comparison the Raman spectra of the length fraction $L_A \approx 580$ nm dispersed using DOC (blue curve) and DNA (red curve). The D-band intensity appears small compared to the G or G' modes and behaves similarly for the two fractions. At 514.5 nm excitation, the SWCNTs are off peak resonance (E_{22}^S or E_{11}^M) for both samples. Slight differences in the excitation energies of the two dispersions in an additional Breit-Wigner-Fano contribution[7] to the G-band from the partial excitation of metallic SWCNTs in the DNA-wrapped sample.

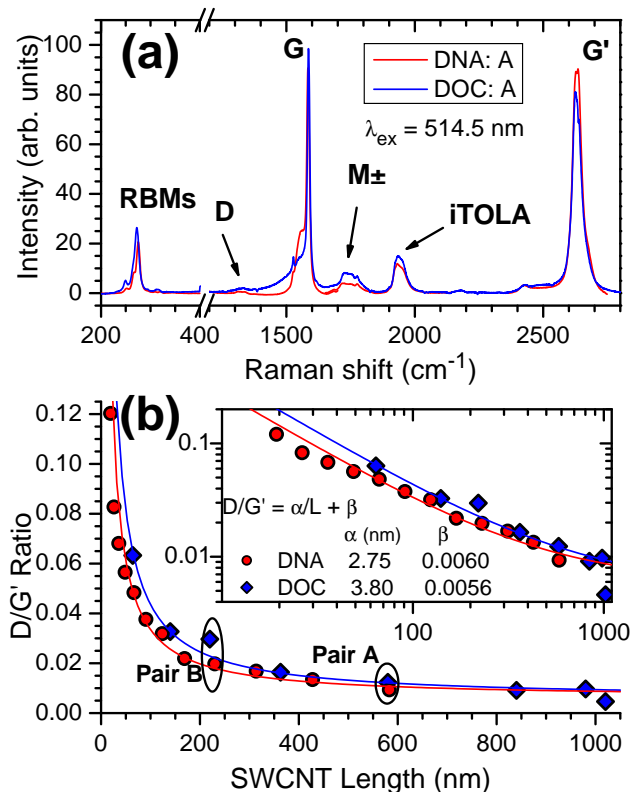


FIG. 2: (a) Raman spectra from the equivalent length $L_A \approx 580$ nm, DOC and DNA dispersed SWCNT fractions with excitation at 514.5 nm. The D-band has similar intensity for the two dispersants. (b) Length dependence of the D/G' ratio for the DNA (red circles) and DOC (blue squares) dispersed SWCNTs. The D/G' (and D/G) ratio for both decreases with increasing SWCNT length. Equivalent length fraction pairs A and B are indicated. Inset: D/G' ratio on a log-log scale.

The quantitative similarity for each of the D, G and G' bands in the two samples shown in Fig. 2(a) is particularly striking. The D-band mode requires in-plane translational symmetry breaking to conserve momentum in a single phonon scattering process.[6] Disorder or defects, including end cap effects, provide the necessary symmetry breaking and give rise to the D-band. The second harmonic of the D-band, G', conserves momentum with two phonons and does not require the presence of defects.

The similarity of D and G spectral features in the equivalent length SWCNTs implies a common degree of disorder for the DNA and DOC dispersions. The presence of disorder/defects strongly affects the recombination of excitons[8] and is thought to be one of the key factors limiting the fluorescence quantum yield.

Thomsen and Reich[9] suggest a comparison of the D/G' intensity ratio as a metric more characteristic of defect density than D/G. Figure 2(b) shows that the ratio of the D-band (≈ 1328 cm⁻¹) compared to G'-band decreases with increasing SWCNT length. DNA (red circles) and DOC (blue squares) dispersants exhibit a common D/G' ratio trend over the entire range of length fractions. In both cases, the D/G' ratio decays towards a small, constant value with an approximately 1/L length dependence. The D/G ratio (not shown) behaves similarly.

Tuinstra and Koenig[10] originally reported the 1/L scaling behavior of the Raman D/G intensity with graphite crystallite size. Cançado *et al.*[11] observed a similar 1/L scaling for graphite nanocrystals studied as a function of excitation energy. A similar 1/L dependence is expected theoretically in SWCNTs for D-band contributions arising from end caps. Such behavior has been observed in short (< 100 nm) SWCNTs.[12] Thus, for defect-free SWCNTs, the contribution from endcaps to the D/G' ratio should scale inversely with length, $D/G' = \alpha/L$, where α is a length-independent constant. As shown in Fig. 2(b), our D/G' ratio closely follows 1/L and then asymptotes to a small, constant value for the longest fractions. Defect density along the nanotube axis should not scale with length and hence provides a constant contribution to the D/G' ratio. Fits of the D/G' ratios to $\alpha/L + \beta$, where β is a constant defect contribution, are shown as solid lines in Fig. 2(b). The length at which the α/L term and the constant term β are equal, represents a crossover between a dominant contribution from endcap defects to those from tube axis defects. The length L_0 at the crossover point, where $\alpha/L_0 = \beta$, may be thought of as a characteristic length between defects. From the fits shown in Fig. 2(b), L_0 is approximately (460 ± 180) nm for DNA and (670 ± 270) nm for DOC. The defect density η is then given by $\eta = 1/L_0$.

The UV-vis transmission spectra of the two sets of length fractions are shown in Fig. 3(a). Apart from a slight red shift of the peak feature locations in the DNA dispersions and the additional absorbance in the UV region resulting from the bound DNA, the absorbance is nearly the same for either dispersing agent. However, as demonstrated in earlier work,[3, 4] the spectral weight of the optical transitions appears to depend on the nanotube length for approximately equal SWCNT concentration. The peak features are appreciably larger for the longer SWCNTs. Figure 3(b) shows the fluorescent emission from the two sets of samples diluted to normalize concentration as determined by the absorption at

775 nm. The fluorescence exhibits a similar length dependence as the absorbance. Note that, the SWCNT fluorescence is approximately 2 – 3 times larger for DOC versus DNA dispersed fractions of the same length. This observation agrees with Haggenueller *et al.*[13] who found DOC-dispersed SWCNTs display the strongest fluorescence among roughly 20 dispersing agents for solutions containing a mix of lengths. The Raman data reported here demonstrate comparable defect density between the two dispersion methods, suggesting that this difference in PL emission with dispersant is an environmental effect.

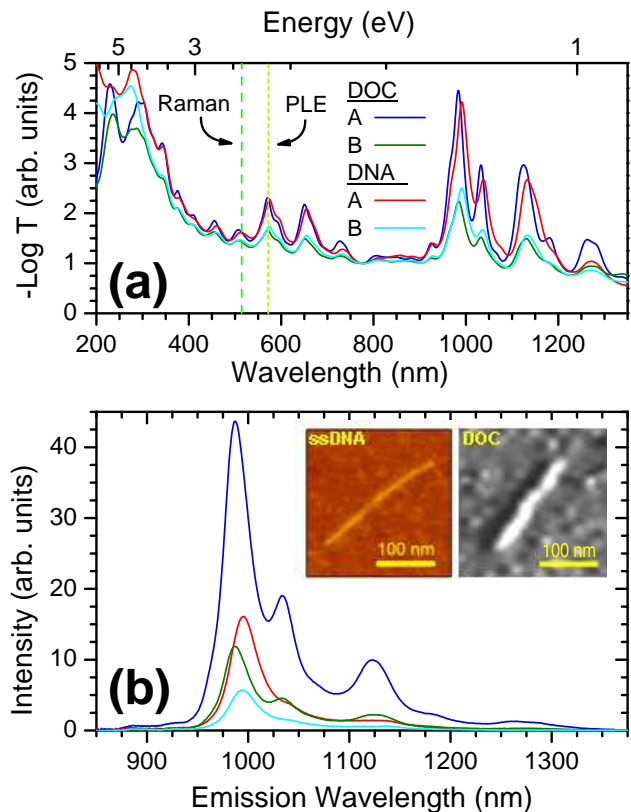


FIG. 3: (a) Log transmission spectra for two sets of SWCNT length fractions with different dispersing agent: ssDNA or DOC. The spectra have been scaled for concentration at 775 nm. Raman excitation at 514.5 nm and fluorescence excitation at 572 nm are indicated with dashed lines. (b) Fluorescence intensity spectra for the samples shown in (a). Inset: Comparison of AFM images for similar length SWCNTs wrapped with ssDNA and DOC. The larger micellar structure formed by the DOC is visible in the micrograph on the right.

Atomic force microscopy (AFM), shown in the inset of Fig. 3(b), reveals a difference in the two surface coatings. The natural tendency for the DOC to encapsulate the SWCNT in a micelle leads to a larger overall diameter of

the entire hydrophilic particle, with less area exposed to the environment. Such a protective layer likely serves to preserve the pristine character of the SWCNT graphitic lattice. In contrast, the DNA physically adsorbs to the surface of the SWCNT in a nonuniform manner. Qian *et al.*[14] found that non-uniform DNA wrapping introduces a localized perturbation on the emission of the SWCNTs, which likely accounts for the reduced PL.

In conclusion, Raman scattering from SWCNTs dispersed with either DNA or DOC depends on length, the D-band contribution results primarily from end caps, and the defect density is approximately equal for the two dispersants. Furthermore, the data suggest that the inhomogeneity of polymer wrapping quenches fluorescent emission from DNA-wrapped SWCNTs as compared to micellar-dispersed SWCNTs. These results will have important implications in biological applications that seek to exploit the intrinsic fluorescent emission of SWCNTs.

Acknowledgments - J.R.S. acknowledges the support of a NIST-National Research Council postdoctoral fellowship.

* jrsimpson@towson.edu

- [1] B. Kitiyanan, W. E. Alvarez, J. H. Harwell, D. E. Resasco, *Chem. Phys. Lett.* **317**, 497 (2003).
- [2] M. Zheng, A. Jagota, E. D. Semke, B. A. Diner, R. S. McLean, S. R. Lustig, R. E. Richardson, N. G. Tassi, *Nat. Mater.* **2**, 338 (2003).
- [3] J. A. Fagan, J. R. Simpson, B. J. Bauer, S. Lacerda, M. L. Becker, J. Chun, K. B. Migler, A. R. Hight Walker, E. K. Hobbie, *J. Am. Chem. Soc.* **129**, 10607 (2007).
- [4] J. A. Fagan, M. L. Becker, J. Chun, E. K. Hobbie, *Adv. Mat.* **20**, 1609 (2008).
- [5] Z. Wu, C. Zhang, P. C. Stair, *Cat. Tod.* **113**, 40 (2006).
- [6] M. S. Dresselhaus, G. Dresselhaus, R. Saito, A. Jorio, *Phys. Rep.* **409**, 47 (2005).
- [7] S. D. M. Brown, A. Jorio, P. Corio, M. S. Dresselhaus, G. Dresselhaus, R. Saito, and K. Kneipp, *Phys. Rev. B* **63**, 155414 (2001).
- [8] L. Cagnet, D. A. Tsyboulski, J. R. Rocha, C. D. Doyle, J. M. Tour, R. B. Weisman, *Science* **316**, 1465 (2007).
- [9] C. Thomsen and S. Reich, *Topics Appl. Physics* **108**, 115 (2007).
- [10] F. Tuinstra and J. L. Koenig, *J. Chem. Phys.* **53**, 1126 (1970).
- [11] L. G. Conçado *et al.*, *App. Phys. Lett.* **88**, 163106 (2006).
- [12] S. G. Chou, H. Son, J. Kong, A. Jorio, R. Saito, M. Zheng, G. Dresselhaus, and M. S. Dresselhaus, *Appl. Phys. Lett.* **90**, 131109 (2007).
- [13] R. Haggenueller *et al.*, *Langmuir* **24**, 5070 (2008).
- [14] H. Qian, P. T. Araujo, C. Georgi, T. Gokus, N. Hartmann, A. A. Green, A. Jorio, M. C. Hersam, L. Novotny, A. Hartschuh, *Nano Lett.* **8**, 2706 (2008).